**Table E1.** Model coefficients for $V_{S30}$-scaling model, $F_v$ and the associated epistemic uncertainty, and for $F_{760}$ and the associated epistemic uncertainty.

| | $F_v$ Median | | | | $F_v$ Uncertainty | | | | | | $F_{760}$ Median | | $F_{760}$ Uncertainty | |
|---|---|---|---|---|---|---|---|---|---|---|---|---|---|---|
| **Period (s)** | $c$ | $V_{ref}$ (m/sec) | $V_1$ (m/sec) | $V_2$ (m/sec) | $V_f$ (m/sec) | $V_1$ (m/sec) | $Vu$ (m/sec) | $\sigma_{VC}$ | $\sigma$ | $\sigma_U$ | $F_{760}$ Impedance | $F_{760}$ Gradient | $\sigma_{F760,imp}$ | $\sigma_{F760,gr}$ |
| -1 | -0.449 | 760 | 331 | 760 | 314 | 200 | 2000 | 0.251 | 0.306 | 0.334 | 0.3753 | 0.297 | 0.313 | 0.117 |
| 0 | -0.290 | 760 | 319 | 760 | 345 | 200 | 2000 | 0.300 | 0.345 | 0.480 | 0.185 | 0.121 | 0.434 | 0.248 |
| 0.01 | -0.290 | 760 | 319 | 760 | 345 | 200 | 2000 | 0.300 | 0.345 | 0.480 | 0.185 | 0.121 | 0.434 | 0.248 |
| 0.02 | -0.303 | 760 | 319 | 760 | 343 | 200 | 2000 | 0.290 | 0.336 | 0.479 | 0.185 | 0.031 | 0.434 | 0.270 |
| 0.03 | -0.315 | 760 | 319 | 810 | 342 | 200 | 2000 | 0.282 | 0.327 | 0.478 | 0.224 | 0.000 | 0.404 | 0.229 |
| 0.04 | -0.331 | 760 | 319 | 900 | 340 | 200 | 2000 | 0.275 | 0.317 | 0.477 | 0.283 | 0.012 | 0.390 | 0.139 |
| 0.05 | -0.344 | 760 | 319 | 1010 | 338 | 200 | 2000 | 0.271 | 0.308 | 0.476 | 0.337 | 0.062 | 0.363 | 0.093 |
| 0.075 | -0.348 | 760 | 319 | 1380 | 334 | 200 | 2000 | 0.269 | 0.285 | 0.473 | 0.475 | 0.211 | 0.322 | 0.102 |
| 0.08 | -0.358 | 760 | 318.38 | 1450 | 333 | 200 | 2000 | 0.268 | 0.281 | 0.472 | 0.512 | 0.237 | 0.335 | 0.103 |
| 0.1 | -0.372 | 760 | 317.13 | 1900 | 319 | 200 | 2000 | 0.270 | 0.263 | 0.470 | 0.674 | 0.338 | 0.366 | 0.088 |
| 0.11 | -0.37410 | 760 | 315.27 | 2000 | 318.41 | 200 | 2000 | 0.26959 | 0.26794 | 0.46303 | 0.72998 | 0.377 | 0.352 | 0.076 |
| 0.112 | -0.37456 | 760 | 314.78 | 2000 | 318.30 | 200 | 2000 | 0.26933 | 0.26887 | 0.46106 | 0.74137 | 0.384 | 0.348 | 0.075 |
| 0.113 | -0.37479 | 760 | 314.52 | 2000 | 318.25 | 200 | 2000 | 0.26918 | 0.26933 | 0.46002 | 0.74742 | 0.388 | 0.345 | 0.075 |
| 0.114 | -0.37503 | 760 | 314.25 | 2000 | 318.19 | 200 | 2000 | 0.26903 | 0.26979 | 0.45894 | 0.75300 | 0.391 | 0.343 | 0.075 |
| 0.115 | -0.37526 | 760 | 313.98 | 2000 | 318.14 | 200 | 2000 | 0.26886 | 0.27024 | 0.45782 | 0.75759 | 0.394 | 0.340 | 0.074 |
| 0.116 | -0.37549 | 760 | 313.70 | 2000 | 318.08 | 200 | 2000 | 0.26868 | 0.27069 | 0.45666 | 0.76065 | 0.397 | 0.338 | 0.073 |
| 0.117 | -0.37573 | 760 | 313.41 | 2000 | 318.03 | 200 | 2000 | 0.26850 | 0.27113 | 0.45547 | 0.76178 | 0.400 | 0.335 | 0.072 |
| 0.118 | -0.37597 | 760 | 313.12 | 2000 | 317.98 | 200 | 2000 | 0.26831 | 0.27157 | 0.45425 | 0.76110 | 0.403 | 0.333 | 0.072 |
| 0.119 | -0.37621 | 760 | 312.82 | 2000 | 317.93 | 200 | 2000 | 0.26811 | 0.27201 | 0.45300 | 0.75894 | 0.406 | 0.330 | 0.071 |
| 0.12 | -0.37645 | 760 | 312.51 | 2000 | 317.88 | 200 | 2000 | 0.26791 | 0.27244 | 0.45171 | 0.75562 | 0.409 | 0.327 | 0.071 |
| 0.125 | -0.37768 | 760 | 310.90 | 2000 | 317.62 | 200 | 2000 | 0.26682 | 0.27456 | 0.44483 | 0.73234 | 0.422 | 0.313 | 0.070 |
| 0.13 | -0.37898 | 760 | 309.19 | 2000 | 317.38 | 200 | 2000 | 0.26565 | 0.27659 | 0.43729 | 0.71641 | 0.434 | 0.299 | 0.070 |
| 0.135 | -0.38036 | 760 | 307.38 | 1800 | 317.15 | 200 | 2000 | 0.26445 | 0.27854 | 0.42916 | 0.66870 | 0.444 | 0.286 | 0.071 |

| | | | | | | | | | | | | | | |
|---|---|---|---|---|---|---|---|---|---|---|---|---|---|---|
| 0.14 | -0.38182 | 760 | 305.51 | 1775 | 316.93 | 200 | 2000 | 0.26325 | 0.28043 | 0.42053 | 0.66026 | 0.454 | 0.273 | 0.070 |
| 0.15 | -0.385 | 760 | 301.63 | 1500 | 316.5 | 200 | 2000 | 0.261 | 0.284 | 0.402 | 0.586 | 0.470 | 0.253 | 0.066 |
| 0.2 | -0.403 | 760 | 279.00 | 1072.91 | 314 | 200 | 2000 | 0.251 | 0.306 | 0.334 | 0.419 | 0.509 | 0.214 | 0.053 |
| 0.25 | -0.417 | 760 | 249.88 | 944.81 | 282 | 200 | 2000 | 0.238 | 0.291 | 0.357 | 0.332 | 0.509 | 0.177 | 0.052 |
| 0.3 | -0.426 | 760 | 224.50 | 867.45 | 250 | 200 | 2000 | 0.225 | 0.276 | 0.381 | 0.27 | 0.498 | 0.131 | 0.055 |
| 0.4 | -0.452 | 760 | 216.50 | 842.72 | 250 | 200 | 2000 | 0.225 | 0.275 | 0.381 | 0.209 | 0.473 | 0.112 | 0.060 |
| 0.5 | -0.480 | 760 | 216.88 | 822.12 | 280 | 200 | 2000 | 0.225 | 0.311 | 0.323 | 0.175 | 0.447 | 0.105 | 0.067 |
| 0.75 | -0.510 | 760 | 226.88 | 814.21 | 280 | 200 | 2000 | 0.225 | 0.330 | 0.310 | 0.127 | 0.386 | 0.138 | 0.077 |
| 0.8 | -0.523 | 760 | 235.00 | 810 | 280 | 200 | 2000 | 0.225 | 0.334 | 0.308 | 0.12 | 0.378 | 0.133 | 0.077 |
| 1 | -0.557 | 760 | 254.75 | 790 | 300 | 200 | 2000 | 0.225 | 0.377 | 0.361 | 0.095 | 0.344 | 0.124 | 0.078 |
| 1.5 | -0.574 | 760 | 275.50 | 805 | 300 | 200 | 2000 | 0.242 | 0.405 | 0.375 | 0.083 | 0.289 | 0.112 | 0.081 |
| 2 | -0.584 | 760 | 296.00 | 810 | 300 | 200 | 2000 | 0.259 | 0.413 | 0.388 | 0.079 | 0.258 | 0.118 | 0.088 |
| 3 | -0.588 | 760 | 311.50 | 819.94 | 313 | 200 | 2000 | 0.306 | 0.410 | 0.551 | 0.073 | 0.233 | 0.111 | 0.100 |
| 4 | -0.579 | 760 | 321.25 | 821.33 | 322 | 200 | 2000 | 0.340 | 0.405 | 0.585 | 0.066 | 0.224 | 0.120 | 0.109 |
| 5 | -0.558 | 760 | 324.25 | 825 | 325 | 200 | 2000 | 0.340 | 0.409 | 0.587 | 0.064 | 0.220 | 0.108 | 0.115 |
| 7.5 | -0.544 | 760 | 325.00 | 819.76 | 328 | 200 | 2000 | 0.345 | 0.420 | 0.594 | 0.056 | 0.216 | 0.082 | 0.130 |
| 10 | -0.507 | 760 | 325.00 | 820 | 330 | 200 | 2000 | 0.350 | 0.440 | 0.600 | 0.053 | 0.218 | 0.069 | 0.137 |

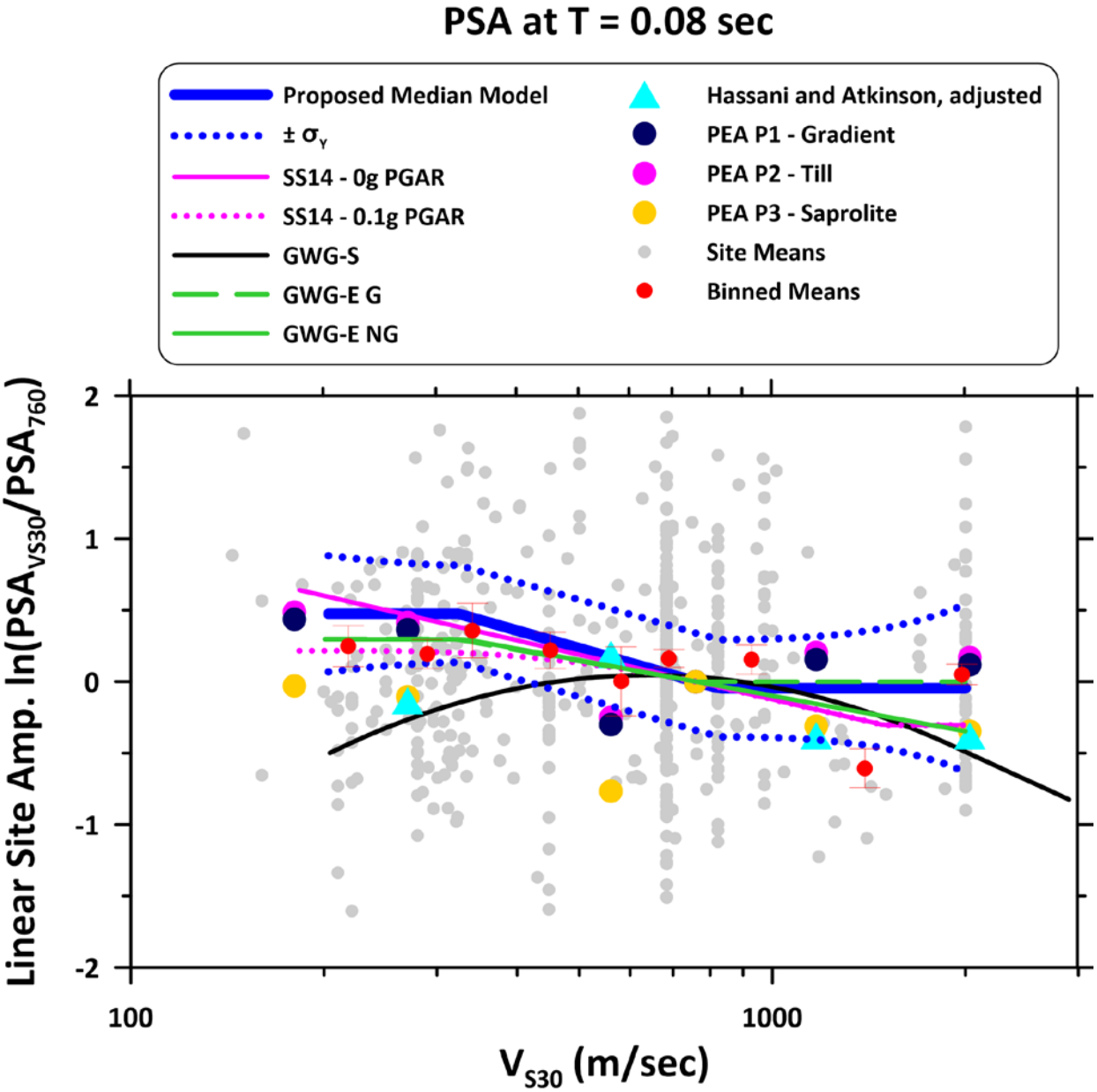


**Figure E1.** Scaling of site amplification with $V_{S30}$ at oscillator period of 0.08 sec, for CENA region from alternate models, and for a reference model for active tectonic regions. SS14 = Seyhan and Stewart (2014) for ATRs, for $PGA_r$ = 0 (linear site amplification only) and for $PGA_r$ = 0.1g (as used for developing current NEHRP site factors). GWG-E G and GWG-E NG = Geotechnical Working Group empirical model for glaciated and nonglaciated regions, respectively (Parker et al. 2019). GWG-S = Geotechnical Working Group simulation-based model (Harmon et al. 2019b). Hassani and Atkinson (2016a,b) = $f_{peak}$-based model for CENA adjusted to unity at 760 m/sec. PEA = Darragh et al. (2015) simulation-based model, adjusted to a reference condition of 760 m/sec using three simulation-based factors for representative $V_S$ profiles (Profile 1 – Gradient, Profile 2 – Till, and Profile 3 – Piedmont Region Saprolite). Means of within-event rock residuals at each site, and their binned means with respect to $V_{S30}$ represent the empirical data considered in GWG-E.

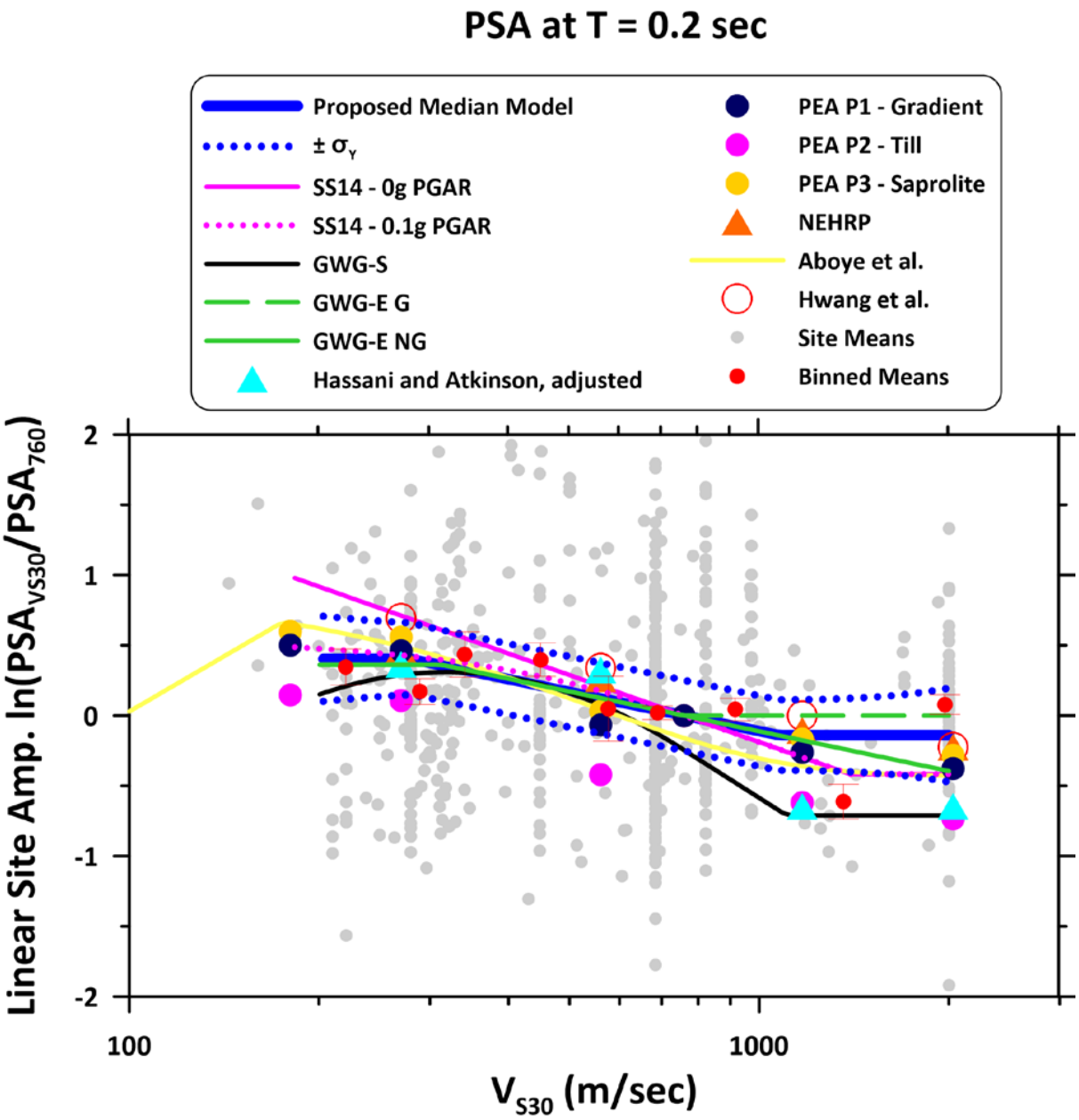


**Figure E2.** Scaling of site amplification with $V_{S30}$ at oscillator period of 0.2 sec. See explanation of figure and symbols in Figure E1 caption.

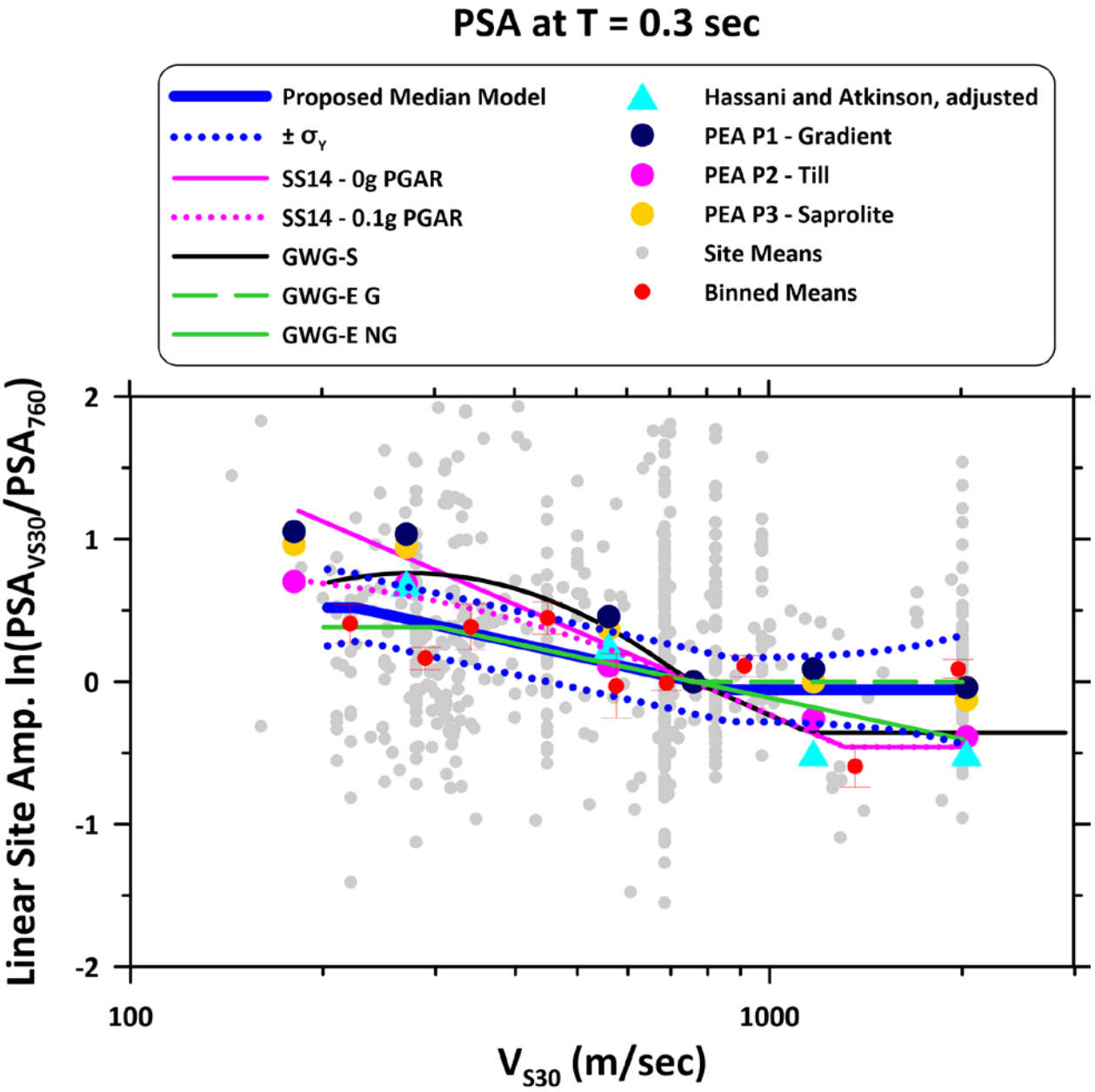


**Figure E3.** Scaling of site amplification with $V_{S30}$ at oscillator period of 0.3 sec. See explanation of figure and symbols in Figure E1 caption.

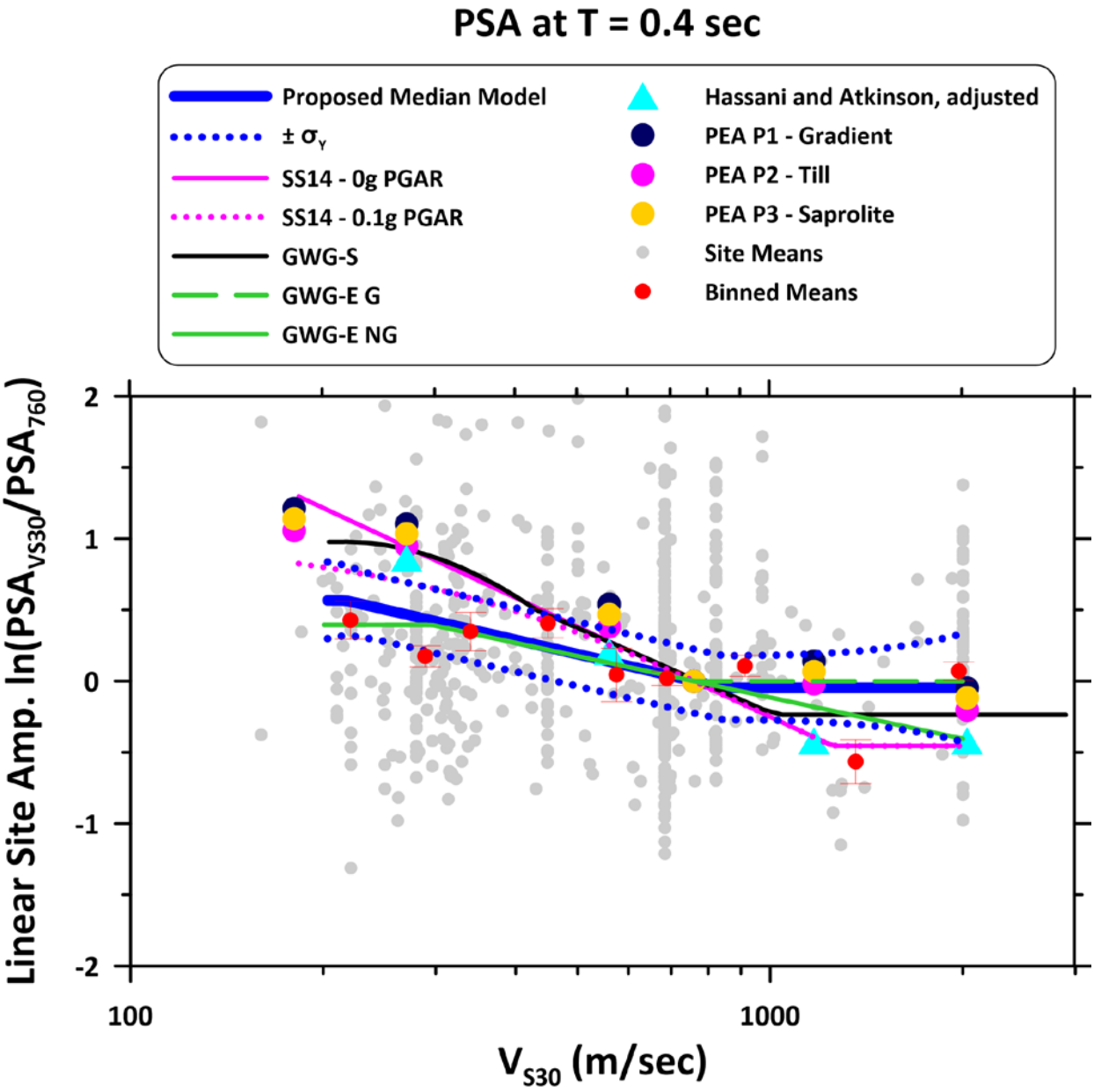


**Figure E4.** Scaling of site amplification with $V_{S30}$ at oscillator period of 0.4 sec. See explanation of figure and symbols in Figure E1 caption.

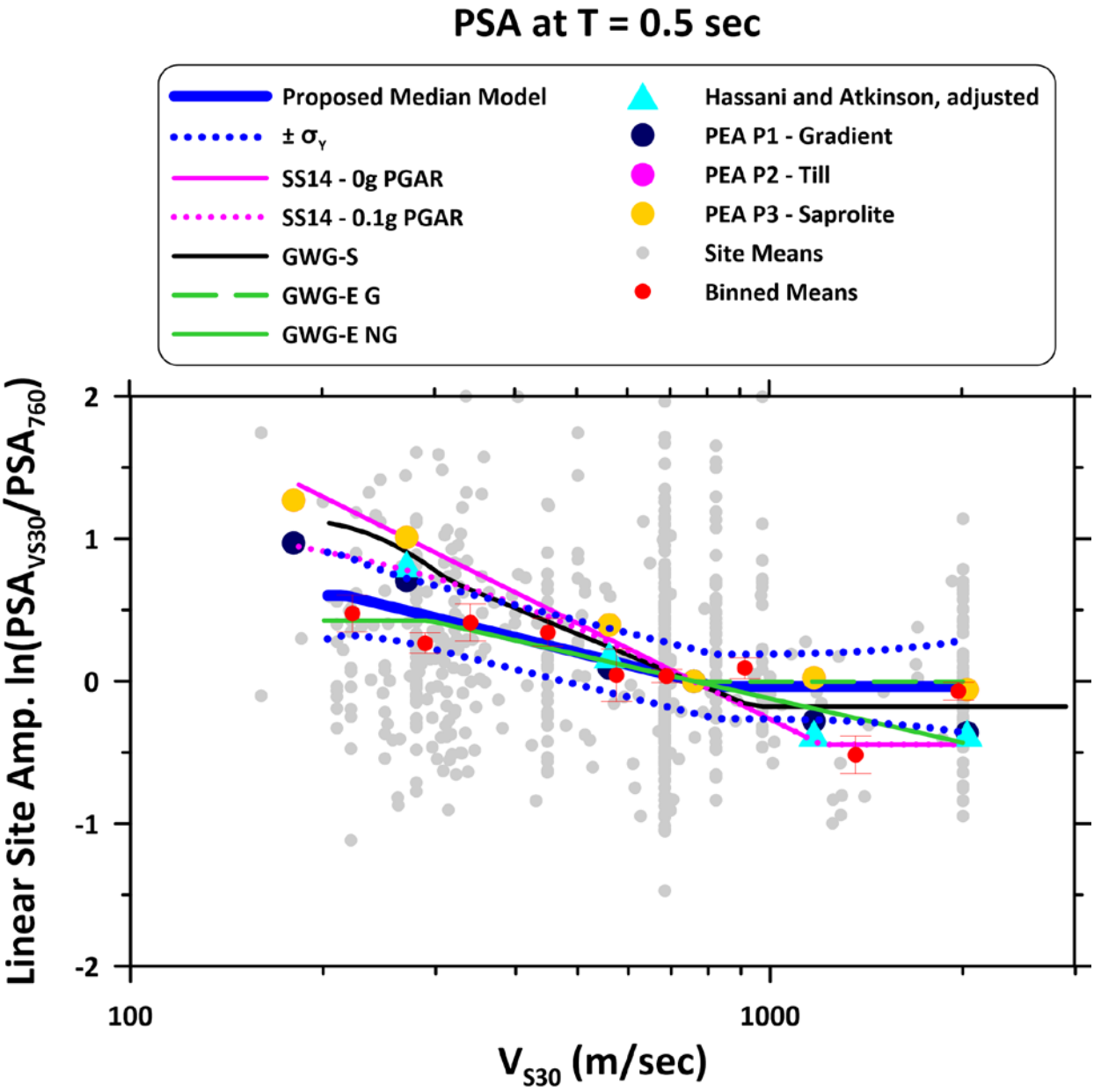


**Figure E5.** Scaling of site amplification with $V_{S30}$ at oscillator period of 0.5 sec. See explanation of figure and symbols in Figure E1 caption.

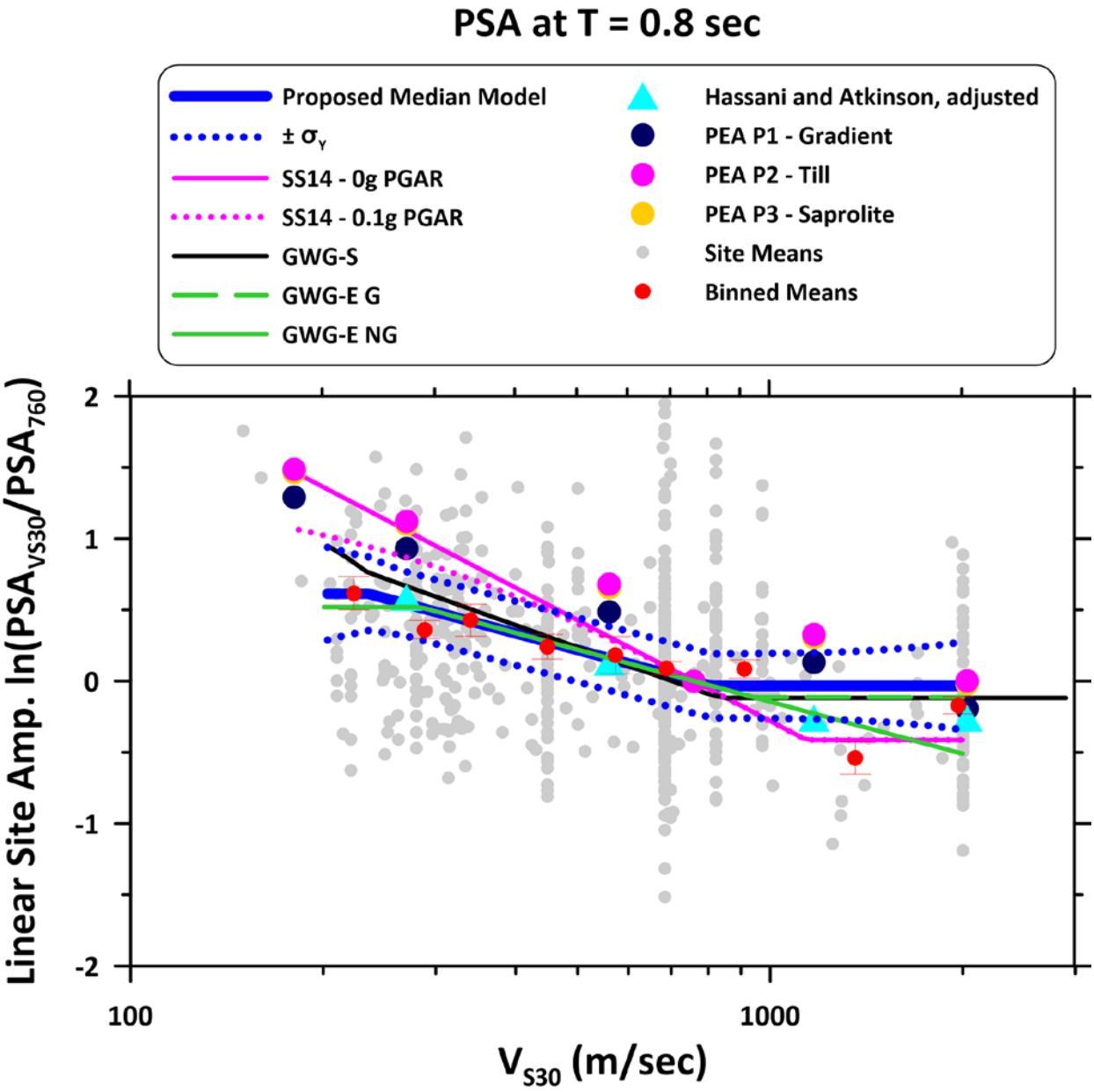


**Figure E6.** Scaling of site amplification with $V_{S30}$ at oscillator period of 0.8 sec. See explanation of figure and symbols in Figure E1 caption.

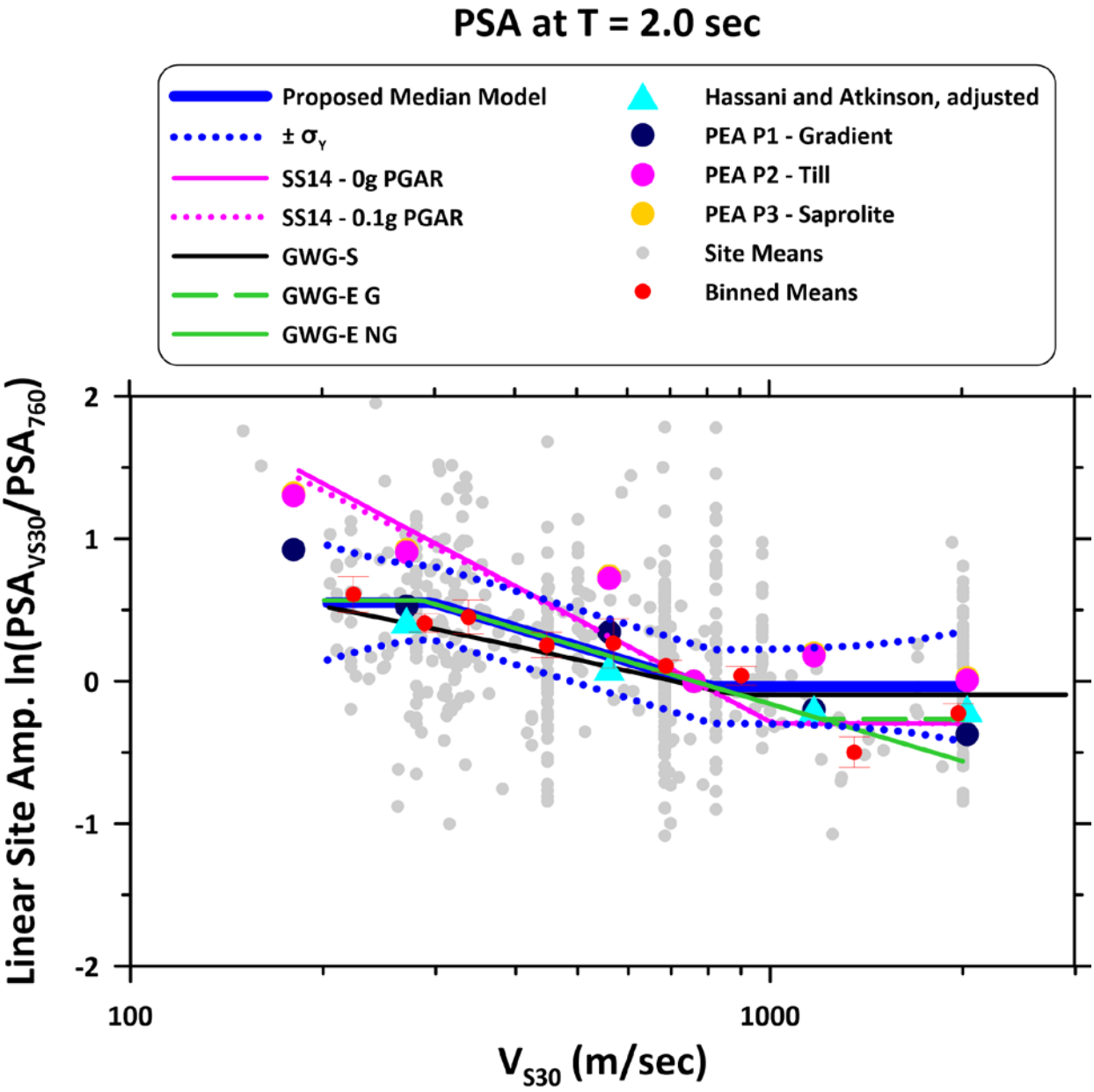


**Figure E7.** Scaling of site amplification with $V_{S30}$ at oscillator period of 2.0 sec. See explanation of figure and symbols in Figure E1 caption.

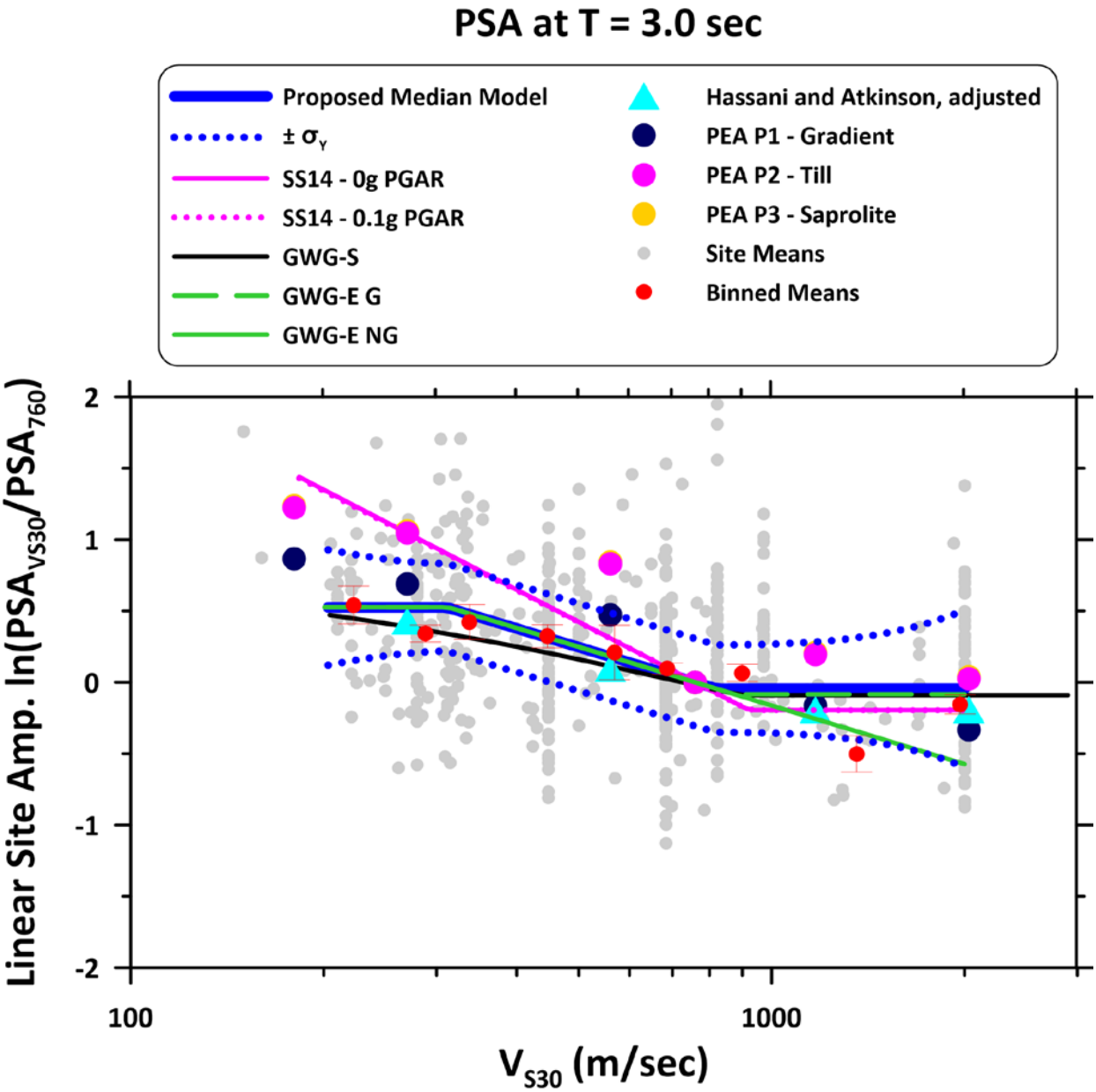


**Figure E8.** Scaling of site amplification with $V_{S30}$ at oscillator period of 3.0 sec. See explanation of figure and symbols in Figure E1 caption.

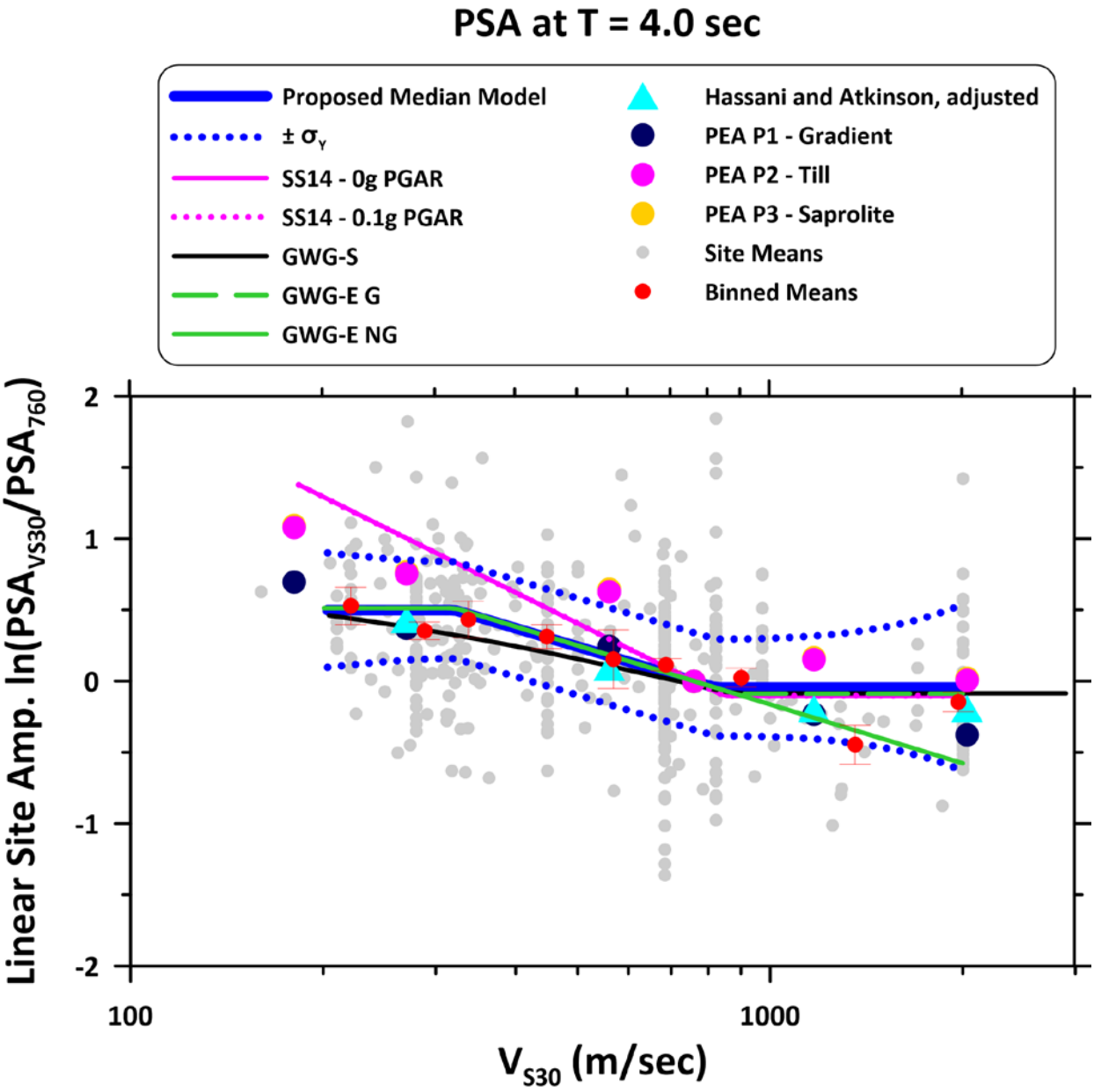


**Figure E9.** Scaling of site amplification with $V_{S30}$ at oscillator period of 4.0 sec. See explanation of figure and symbols in Figure E1 caption.

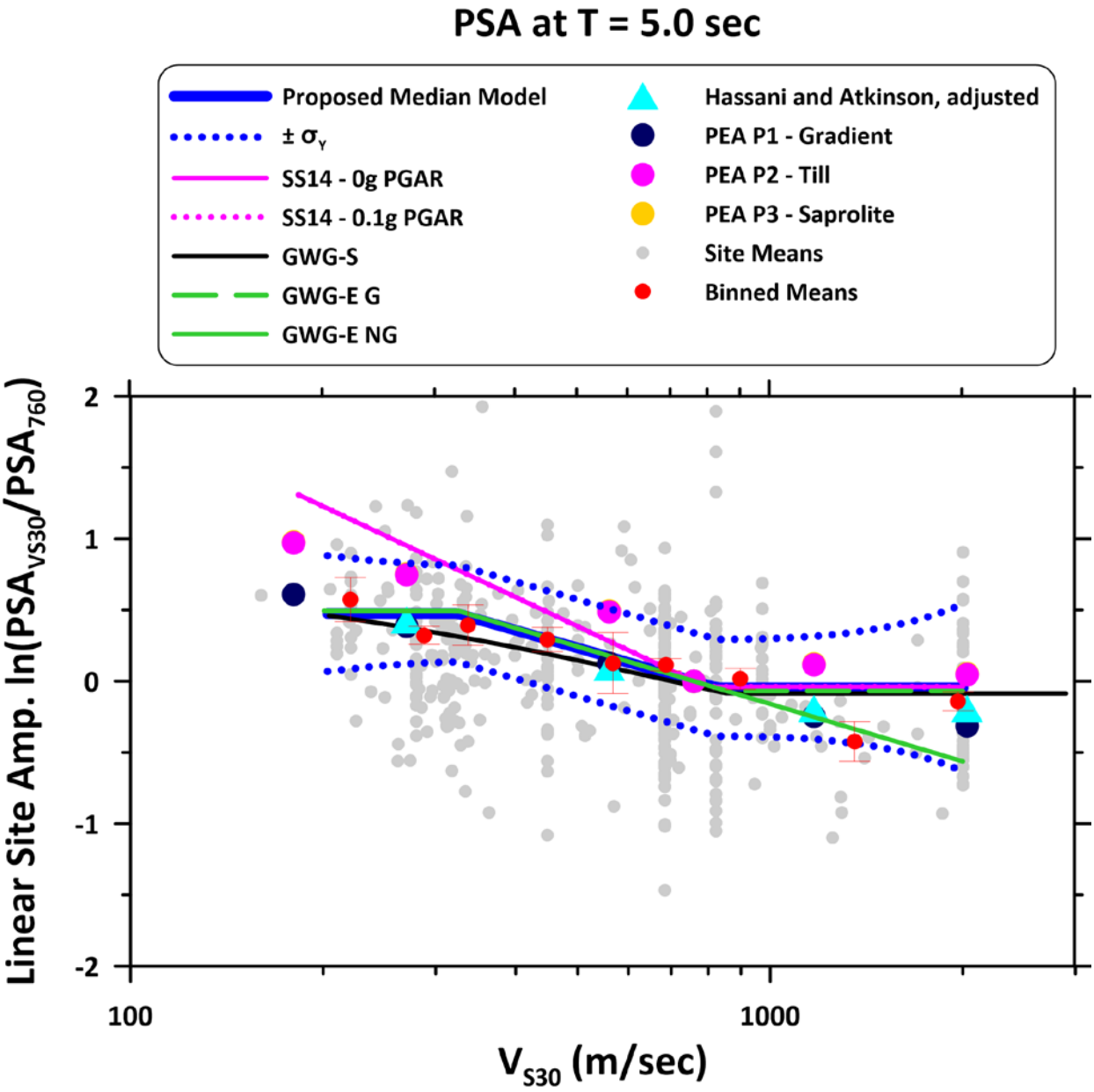


**Figure E10.** Scaling of site amplification with $V_{S30}$ at oscillator period of 5.0 sec. See explanation of figure and symbols in Figure E1 caption.

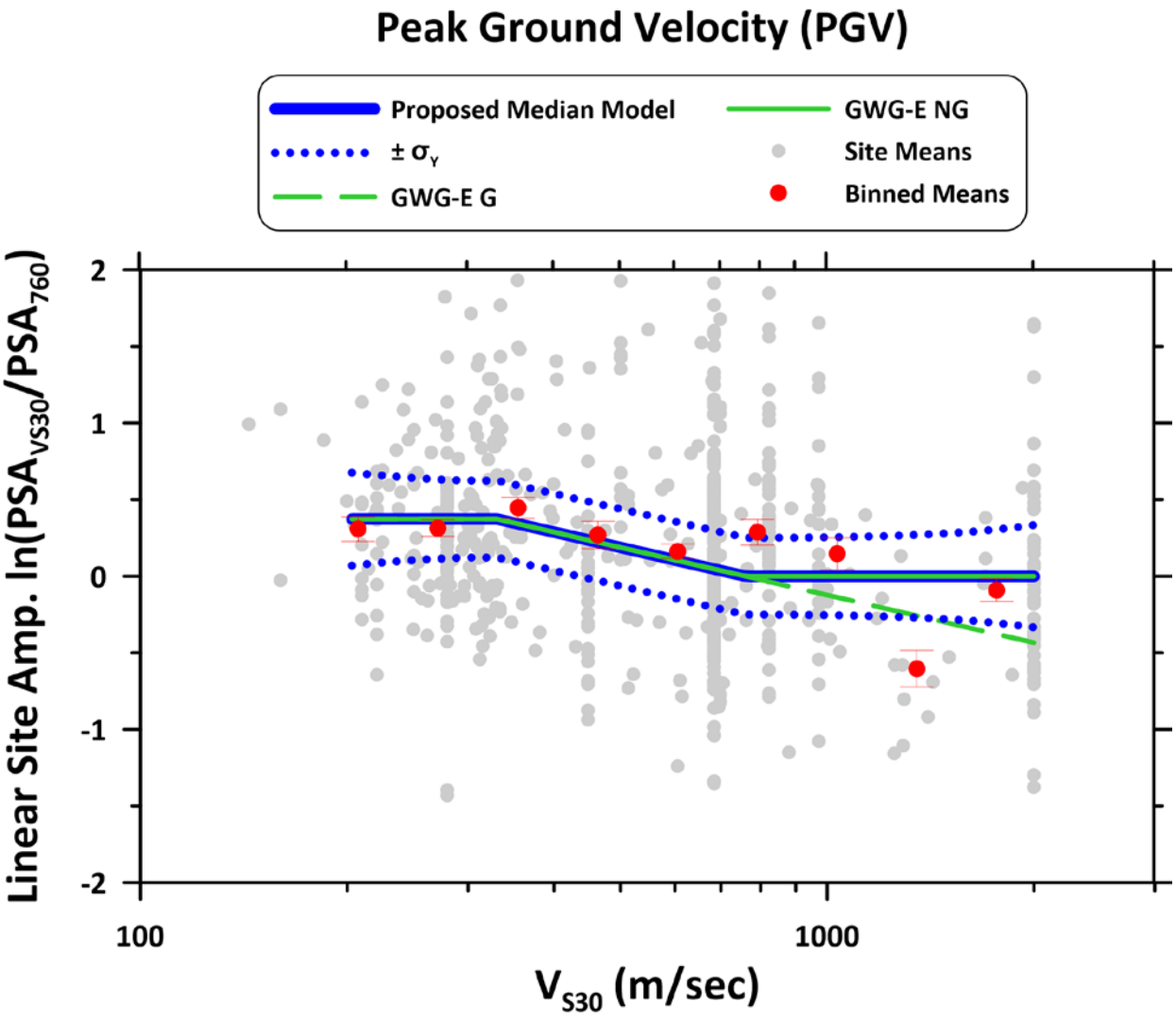


**Figure E11.** Scaling of site amplification with $V_{S30}$ at peak ground velocity (PGV). See explanation of figure and symbols in Figure E1 caption.